

1 Original research paper

2

3 Vehicular emission approximation using wavelet 4 analysis

5

6 Mahbuba Khan¹, Fengxiang Qiao, Ph.D^{1,*}, Lei Yu, Ph.D., PE.¹,

7

8 ¹*Department of Transportation Studies, Texas Southern University, 3100 Cleburne Avenue,*
9 *Houston, TX 77004*

10

11 **Abstract**

12 Vehicular emission has been recognized as one of the major sources of air pollution as
13 such emissions contain harmful greenhouse gases. Hence processing of air pollution data
14 has gained interest which, in turn, made decomposition and transformation algorithms to
15 be important tools in data analyses. For analyzing vehicular pollution, the key variables are
16 the speed, acceleration and pavement roughness. Presently, portable emission
17 measurement system (PEMS) can be employed to collect on-road gas emission data for
18 every second and smartphone apps such as Roadroid are used to estimate road
19 roughness. Although analytical modeling can provide average estimation on the behavior
20 of roughness and how it affects the emission, numerical transformation and decomposition
21 can offer superior approximation since these techniques sweep the whole spectrum of
22 available data. This paper presents a discrete wavelet transformation procedure and
23 discusses the low frequency components of the analysis to approximate the relation

24 between pavement roughness and gas emissions. Here, PEMS data of several road
25 segments from greater Houston were considered. These road segments, selected as
26 testing sites, are approximately 550 km of length in total. The emission data obtained from
27 PEMS in these sites for various gas exhaust such as CO₂, CO, NO_x, and HC and fuel
28 consumption (FC) are decomposed by Multilevel 1-dimensional discrete wavelet analysis
29 to analyze the wavelet approximations of emission and the underlying trends. The results
30 of this literature can assist in the prediction of vehicular emission for different pavement
31 conditions.

32

33 **Keywords:**

34 Discrete wavelet transformation, approximation analysis, wavelet decomposition, pavement roughness,
35 vehicular emission

36

*Corresponding author. Tel.: 713-313-1915, Fax: 717/313-1856
E-mail: qiao_fg@tsu.edu (Fengxiang Qiao, PhD, Professor).
yu_lx@tsu.edu (Lei Yu, Ph.D., PE., Professor)
mahbubamouree@gmail.com (Mahbuba Khan, Graduate Research Assistant)

37 1 Introduction

38 Vehicular emission is one of the major contributors to air pollution and, thus, a risk for human health as
39 well as for the environment. According to the National- Level Greenhouse Gas Inventory of EPA (2016),
40 transportation sector is accounted to be the second largest portion of U.S. greenhouse gas emissions in
41 2014 contributing 26% to it. A report from the Massachusetts Institute of Technology's (MIT) Laboratory
42 for Aviation and the Environment in 2013 presents that every year in the USA 53,000 early deaths occur
43 due to vehicle pollutants (Caiazzo 2003). Carbon dioxide (CO₂), carbon monoxide (CO), nitrogen
44 oxides (NO_x), hydrocarbons (HC) etc. are the most malevolent gasses emitted by vehicles while in use.
45 Identifying the causes that trigger the vehicular emissions and then modelling the emission to estimate
46 accurately for planning emission control is necessary as they pose high risk to the environment and
47 longer also, human health (Li 2015).

48 The several factors that could be responsible for influencing the type and amount of gas emissions on
49 the road are vehicle type, ambient temperature, vehicle age, fuel type, and vehicle speed. Nabi et al.
50 (2016) showed that activities such as changing lanes may have impact on vehicular emission and fuel
51 consumption. But there could be another factor, pavement roughness, affecting vehicle speed and
52 acceleration. Although speed and acceleration directly affect emissions, it is generally assumed that
53 roadway pavement roughness might not directly affect gas emission rates as much as speed and
54 acceleration, but the combined effect might be highly notable. Thus, studies have been conducted to
55 explore the effect of road roughness on vehicular emission. One study indicated a slight decrease in the
56 CO₂ emission from roads in poor conditions to roads in either fair or good condition (Kalembo 2012).
57 Another study from Greene, Suzanne et al (2013) revealed a linear increase of fuel consumption with
58 respect to roughness index for different types of vehicles. Both researches suggested that driving on
59 rough roads consumes more fuel and produces more vehicular emission than driving on smooth roads.
60 In order to assess its impact, the international roughness index (IRI) was invented as a common index
61 for profile measurements of the road surface. It measures roughness that is based on the simulated
62 response of a generic motor vehicle to the roughness in a single-wheel path of the road surface. The IRI
63 was developed by the World Bank in the 1980s and has been identified as a primary factor to indicate

64 the condition of pavement (Papageorgiou 2014).

65 Portable emission measurement system (PEMS) is one of the most common and effective methods to
66 collect on-road emission data. The PEMS can measure emissions from an engine's combustion so that
67 the real-world in-use testing condition can be identified. It accurately measures gas emissions such as
68 CO₂, CO, NO_x, and HC as well as fuel consumption for each second while the vehicle or the equipment
69 are in use.

70 Wavelet transform or wavelet analysis is a very useful mathematical tool for frequency analysis as it
71 has overcome the limitations of Fourier transform. Wavelets are a type of function that is used for
72 confining a given function in both position and scaling (Veitch 2005). Fundamentally, the wavelet
73 transform can decompose a signal into several frequency features and then presents each of them with
74 a product matched to its scale (Wei 2002). It has been used widely in various other fields involving
75 computation such as computing, biology, and statistics especially for signal processing, image
76 compression, subband coding, and sound synthesis. However, several recent studies have been
77 successfully utilized this tool in the area of transportation research as it is proficient of analyzing
78 complicated mathematical function. Wei et al. (2005) suggested that wavelet analysis can present
79 detailed information of road roughness that is useful to maintenance operations, detection of pavement
80 surface deterioration, and the trend of roughness deterioration. Another research of Wei et al. (2004)
81 showed that wavelet transform can characterize detailed features of pavement roughness of different
82 wavelengths quantitatively with regard to wavelet energy. Zhao et al. (2006) proposed a wavelet-based distress
83 detection, isolation and evaluation which can be a useful index for pavement inspection and distress evaluation. In
84 an advanced research, Wang et al. (2014) developed a model incorporating wavelet neural network and genetic
85 algorithm that can predict the distribution of air pollution in real-time near road intersections. This research is
86 motivated by these previous studies where transformation techniques such as wavelet analysis were employed in
87 the field of pavement studies, whereas we intend to use it to reveal the complicated relation between pavement
88 roughness and vehicular emission.

89 **2 Research Objective**

90 The goal of this research is to evaluate the relationship between pavement roughness and vehicular

91 emission through performing multilevel discrete wavelet analysis on the gas emission and fuel
92 consumption data collected during test drive. The results will be later validated by comparing with
93 another curvilinear analysis. During wavelet analysis and subsequent sections, each type of emission
94 data for all the road segments will be sorted according to the ranges of VSP (vehicle specific power) and
95 then decomposed individually in order to be analyzed based on the approximations. Successful
96 outlining of the dependency of vehicular emission on pavement roughness and its validation are
97 expected to be the outcome of this analysis. These findings can be utilized later for roadway designing
98 and planning to decrease vehicular emissions due to roughness.

99 **3 Wavelet Transformation**

100 Wavelet transform or analysis is the study on how a particular function is varying over time by finding a
101 suitable wavelet function that matches with the given function with the variation of scales and position
102 (Qiao 2003). The wavelet transform can be divided into two types: continuous wavelet transform (CWT)
103 and discrete wavelet transform (DWT) based on whether the scale can be continuously taken or in a
104 discrete manner.

105 Each wavelet is derived from a function ψ , which is generally referred to as the “mother wavelet” from
106 two linear transformations that determine the width of the window and hence define the resolution of the
107 transform as given in Eq. (1) (Daubechies 1992).

$$108 \quad \psi_{s,u}(x) = \frac{1}{\sqrt{s}} \cdot \psi\left(\frac{x-u}{s}\right) \quad (1)$$

109 where, s and u are scale parameters for dilation and translation, correspondingly.

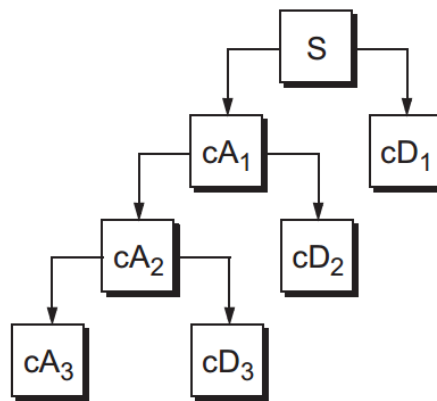
110 The wavelet transform of a function $f(x)$ for a given resolution (s, u) is then given as Eq. (2)
111 (Daubechies 1992).

$$112 \quad WT_{s,u}\{f(x)\} = \int_{-\infty}^{+\infty} f(x) \cdot \frac{1}{\sqrt{s}} \cdot \psi^T\left(\frac{x-u}{s}\right) dx \quad (2)$$

114 **3.1 One-Dimensional Discrete Wavelet Analysis**

115 There is one independent variable and one corresponding dependent variable in 1D wavelet analysis. It
 116 is effective to calculate wavelet coefficients of the dependent variable by choosing a subset of scales
 117 and positions of the independent variable rather than at every possible scale, which would, in turn,
 118 produce a huge amount of data (Qiao 2006). This analysis can be obtained from the discrete wavelet
 119 transform (DWT). In DWT, there are two relative terms: “approximations” and “details.” The
 120 “approximations” are the high-scale, low-frequency components of the signal, while the “details” are the
 121 low-scale, high-frequency components.

122 The decomposition process can be iterated, with successive approximations being decomposed in
 123 turn, so that one signal is broken down into many lower resolution components. This is called the
 124 wavelet decomposition tree. For example, a 1D signal $s[n]$ is passed through a series of stages
 125 consisting of one high-pass and one low-pass filters in order to realize 1D-DWT. During each stage
 126 (also known as levels), the filter outputs are subsampled by 2. The process is shown in Fig 1. Where, A_1
 127 and D_1 denote impulse functions through Level 1 low- and high-pass filters, respectively.



128
 129 **Fig. 1** Wavelet Decomposition Tree

130 We can continue this process for further levels shown in Eq. (3).

$$\sum_{k=-\infty}^{\infty} s[k] a_1[2n - k] = A_1[n] \xrightarrow{\text{Level 2}} \sum_{k=-\infty}^{\infty} A_1[k] a_2[2^2 n - k] + \sum_{k=-\infty}^{\infty} A_1[k] d_2[2^2 n - k] \quad (3)$$

132

133 This process can be repeated for level m , and we will have one “approximation” signal A_m along with

134 m-numbers of “details” signals, namely, $D_m, D_{(m-1)}, D_{(m-2)}, \dots, D_2, D_1$. As shown, the decomposition
135 process can be iterated, with successive approximations being decomposed in turn, so that one signal
136 $s[n]$ is broken down into $m+1$ lower-resolution components. These components are then analyzed to
137 reveal the nature and characteristics of the original signal.

138 **4 Test Description**

139 Several road segments of different length were selected to collect on-road data in greater Houston and
140 are 422.66 km of length in total. The selected pavements are asphalt and were due to be treated at the
141 time of test. The testing period was from May 1, 2015, to June 11, 2015, for the period of nonpeak hours
142 during dry weather conditions (Average temperature was 84°F with an average humidity of 68%). To
143 maintain the integrity in driving behavior and pattern and also similar outputs of vehicular activities, one
144 dedicated driver and vehicle were in service to conduct all the field tests. The vehicle was a light-duty
145 gasoline vehicle: a 2004 Subaru Forester.

146 The PEMS was installed inside the vehicle and connected to the engine through three types of
147 sensors: temperature, air-pressure, and RPM (Rotation Per Minute) sensors. When the vehicle was in
148 use, the PEMS accurately recorded time, RPM, intake air temperature, air pressure, emission
149 concentrations of CO_2 , CO, HC, and NO_x and speed for every second. Also, coordinates (latitude,
150 longitude, and altitude) of the location for each second were obtained using Global Positioning System
151 (GPS). An Android app called Roadroid was used to measure the roughness of the road the vehicle was
152 driven on. Roadroid provides IRI data obtained by smartphone accelerometer and GPS-photo of the
153 road, which is later highly correlated with the roughness measured by the Laser IRI surveys (Forsl6f
154 2013). Then the app server wirelessly transfers the collected data to an internet mapping server with
155 spatial filtering functions which makes the datasets highly reliable. A cell-phone with that app installed
156 was mounted in the front of the vehicle, and the app was turned on the entire time of testing. The
157 Roadroid can provide two options of IRI: a) estimated IRI (eIRI) and b) calculated IRI (cIRI) (Forsl6f
158 2015).

159 **5 Data Processing**

160 PEMS produces data for CO₂, CO, NO_x, and HC and fuel consumption in time dependent manner such
161 as gram/second or milligram/second whereas the IRI data are in the space domain (m/km). Therefore,
162 the emission rates obtained directly from the PEMS were converted into emission factors (gram/meter
163 or milligram/meter) for every 5 meter. Roadroid provides two types of IRI data: a) estimated IRI (eIRI)
164 and b) calculated IRI (cIRI). The setup for eIRI is assumed to compensate for speed in a relatively larger
165 range (20-100 km/hr) than cIRI which can accommodate narrower speed range such as 60-80 km/hr.
166 The value of eIRI shows more consistency considering this factor and therefore, was used in this
167 analysis. Vehicle specific power (VSP) is a function of speed and acceleration rate which was estimated
168 from the instantaneous speed data acquired from PEMS. VSP for light duty vehicles was estimated by
169 using the Eq. (4), as proposed by Jimenez–Palacios et al. (1998).

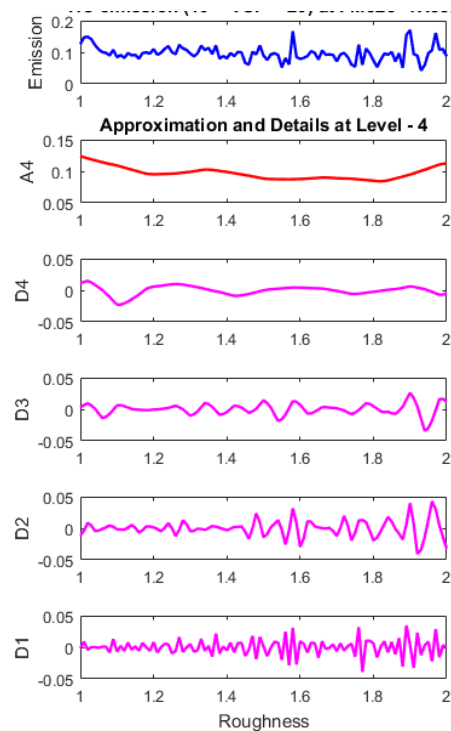
$$170 \quad VSP = v \times (1.1a + 9.81 \times \text{grade}\% + 0.132) + 0.000302v^3 \quad (4)$$

171 where, v is the vehicle speed (m/s), a is the acceleration (m/s²) and grade is the vehicle's vertical rise
172 divided by slope length which can be assumed to be zero if the terrain is flat.

173 The data points were uniformly spaced for sampling to decompose. In addition, data were binned into
174 four VSP ranges: $VSP < 0$, $0 < VSP < 10$, $10 < VSP < 20$ and $VSP > 20$, to reduce the number of
175 independent variables. The emission versus roughness data for each VSP range were collected and
176 then sorted and interpolated in uniform data points. Although the PEMS data contains a large variation
177 of both VSP and roughness, it was found that, the acceptable range of VSP is no less than -10 and no
178 more than 30. IRI data were interpolated within a range of 1 m/km to 3 m/km having an interval of 0.01
179 m/km per the spreading of data points. Next, multi-level discrete wavelet analysis was performed using
180 built-in MATLAB functions. Among the various types of wavelets, haar, Daubechies of order N (db N),
181 and Symlets of order N (sym N) possess the properties required for simple discrete wavelet analysis.
182 Although, above mentioned three types of wavelets were applied initially to decompose the data set but
183 finally, "sym4" was used due to the minimum error.

184 The analysis provides the approximations of level 2 for all the gasses and FC for all VSP ranges. For
185 the sake of discussion, an example of wavelet analysis of level 4 is showed in Fig. 2. Here, the
186 approximation is denoted by A4 and it shows follows the trend of the original data. Emission factors or
187 rates can be predicted using the approximation and thus, identifying the cause of emission features and

188 finding a probable solution of such emission occurring due to uneven pavement. The level 4 analysis
189 also provides four two high-frequency components and two other low-frequency components. These
190 frequency subbands combined with percentage of energy associated with each subband can reveal the
191 lead contributor behind vehicular emission on road (Khan 2017). Although, the level of the analysis can
192 be further increased, but an excessive level will not be able to provide any additional information; rather
193 it will only burden computational labor.



194
195 **Fig. 2** 1D discrete wavelet analysis to decompose one emission (mg/m) versus roughness (m/km) data

196 **6 Result and Discussion**

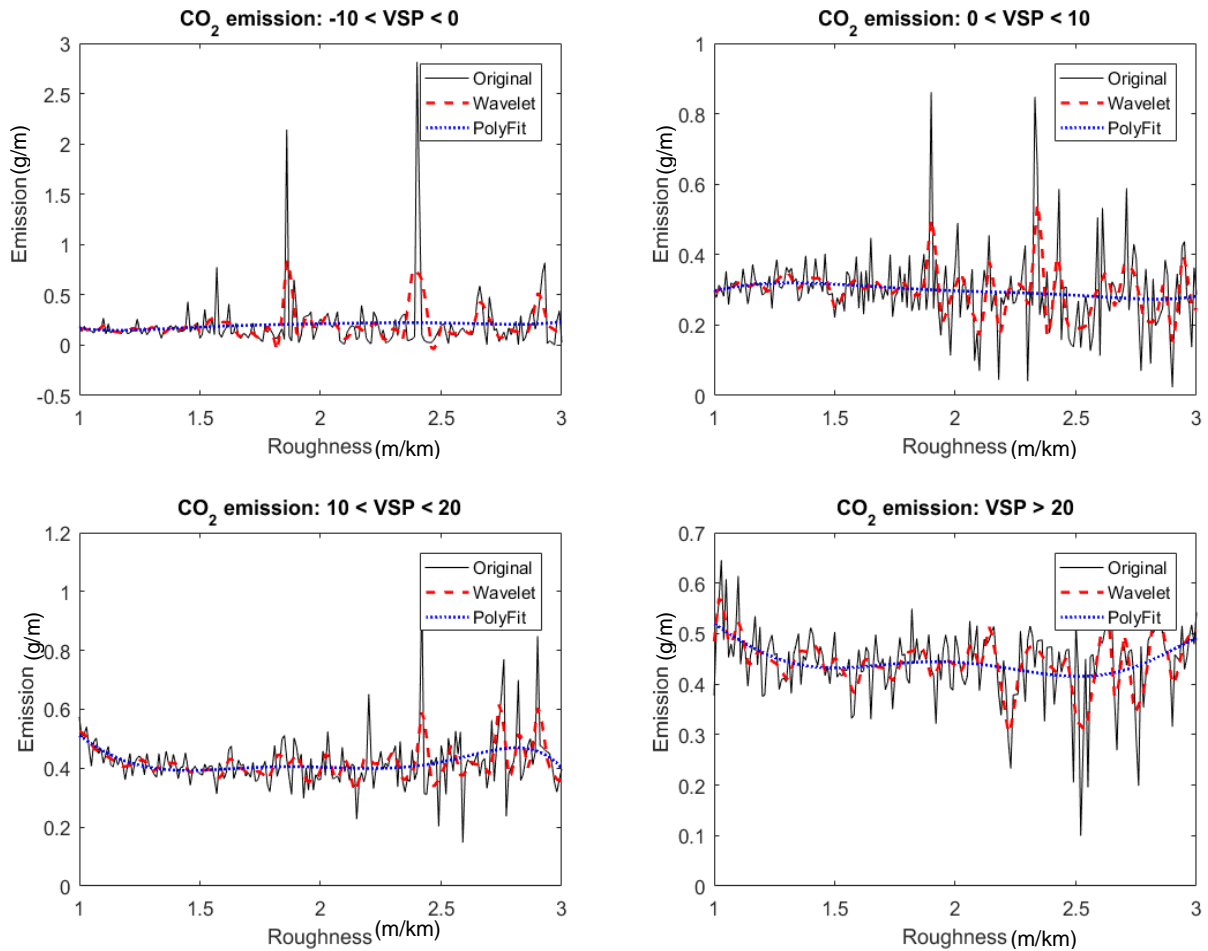
197 One major advantage offered by wavelets is the ability to perform local analysis—that is, to analyze a
198 localized area of a larger signal due to its adaptive solving methods (Nagy 2015). Therefore, wavelet
199 analysis is capable of revealing aspects of emission versus roughness data that other signal analysis
200 techniques (such as Fourier Analysis) miss-aspects such as emission trends, breakdown points, and
201 how emission changes for a small or large change of roughness. Furthermore, wavelet analysis
202 inherently compresses large sets of data and is capable to de-noise a signal to reveal simplified
203 approximations without degrading the signal itself. In this literature, the emission versus roughness data

204 for a particular range of VSP are decomposed and analyzed using 1D wavelet analysis.

205 *6.1 Wavelet Analysis of Gas Emissions and Fuel Consumption versus Roughness*

206 As discussed above, the analysis on current data sample is limited in 2-level analysis for evaluating the
207 approximations. This is because higher level of approximations will only lose data trend and thus, is
208 detrimental for the purpose of this study. Now, multilevel 1D wavelet analysis is performed on CO₂, CO,
209 HC, and NO_x emission data collected from the selected road segments in order to decompose the data.
210 Then the approximation is analyzed to understand the pattern and trend of the emissions and fuel
211 consumption for each VSP range. The data for each emission were also fitted to Polynomial curvature of
212 order 6. The Polyfit and Wavelet results were then compared to find out the best analysis.

213 Fig. 3 shows the comparison among original, wavelet and PolyFit data of CO₂ emission for the four
214 different VSP ranges. The first sub-figure shows that the CO₂ emission has sharp peaks leading to 2 –
215 3 mg/m emission for negative VSP regime. For positive VSP, the maximum values of peaks are below 1
216 mg/m. It is evident from the figures that wavelet analysis is superior in approximating the experimental
217 data than the polynomial fitting. While the polynomial fitting can only follow the general trend of the data,
218 wavelet approximation captures the sudden rise and fall observed in PEMS data as well. This enables
219 wavelet analysis to be a better candidate in approximating emission vs roughness trends for untested
220 pavements.



221

222

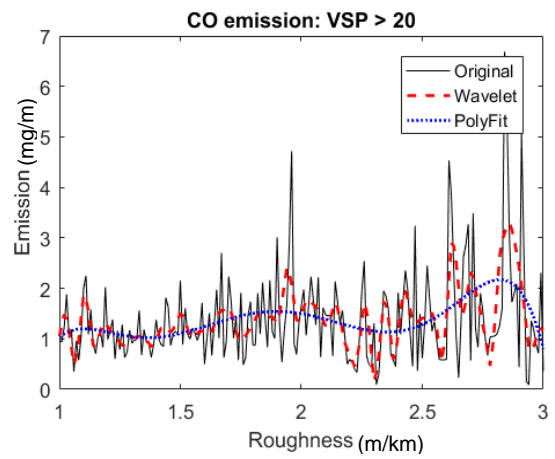
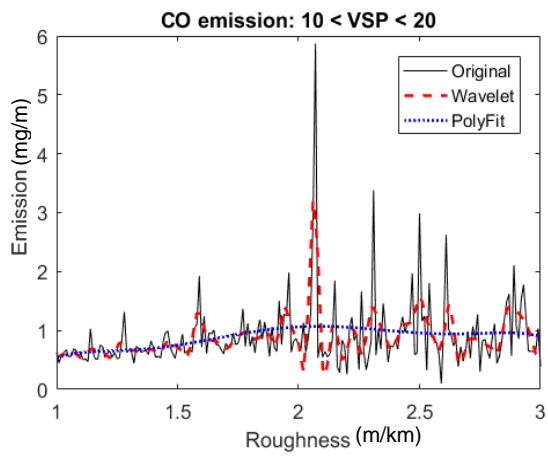
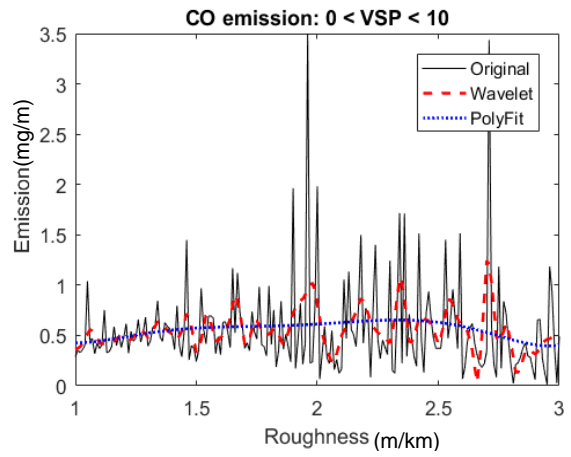
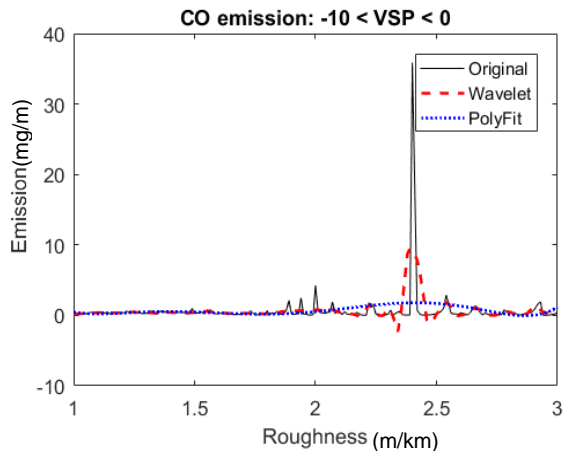
Fig. 3 Comparison between Wavelet Approximation and Polyfit of CO₂ emission for different VSP ranges

223

Similarly, Fig. 4, 5, 6 and 7 show the comparison among original, wavelet and PolyFit data of CO, HC, NO_x emission and FC correspondingly for the four different VSP ranges. All of them have very sharp peaks for negative VSP than the other VSP ranges. A distinct superiority of wavelet analysis is visible in all the figures in case of approximating the original data over polynomial fitting. Following the analysis of CO₂, the other analysis also imply that the polynomial fitting can only follow the general trend of the data, whereas wavelet approximation captures the details of sudden rise and fall observed in PEMS data as well. Therefore, overall analysis qualifies wavelet analysis to be a better candidate in approximating emission vs roughness trends for untested pavements.

229

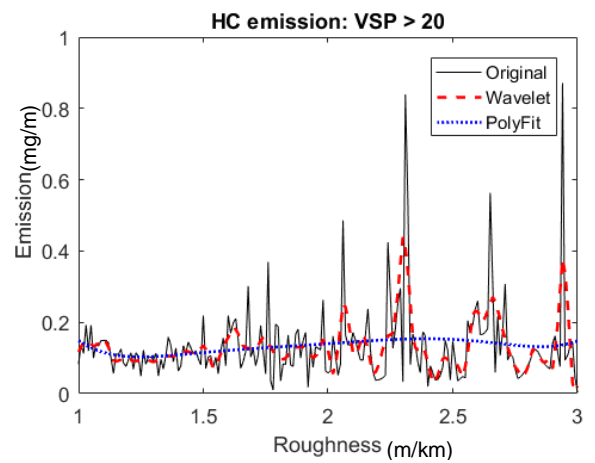
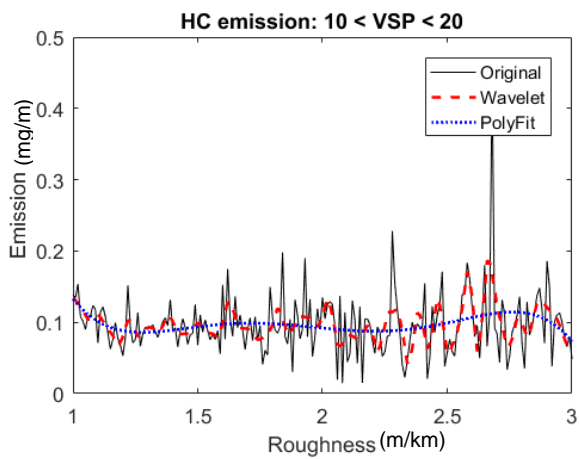
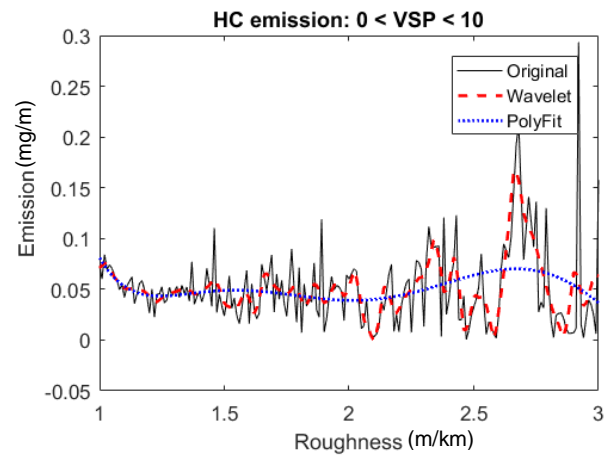
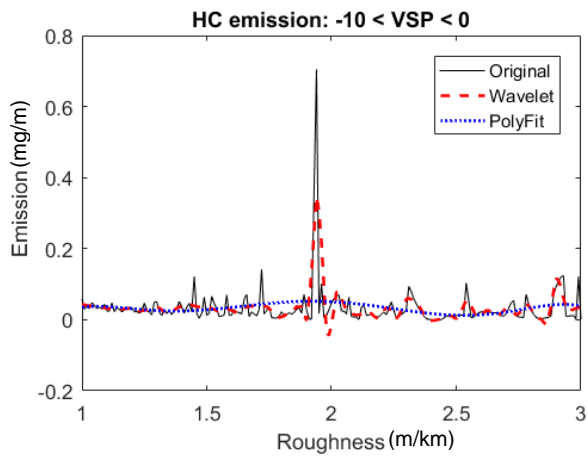
230



231

232

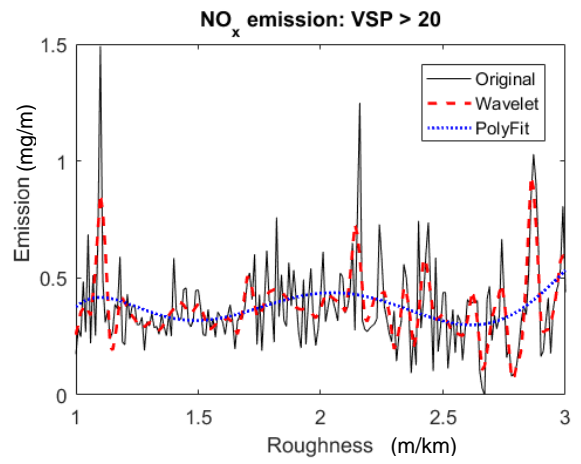
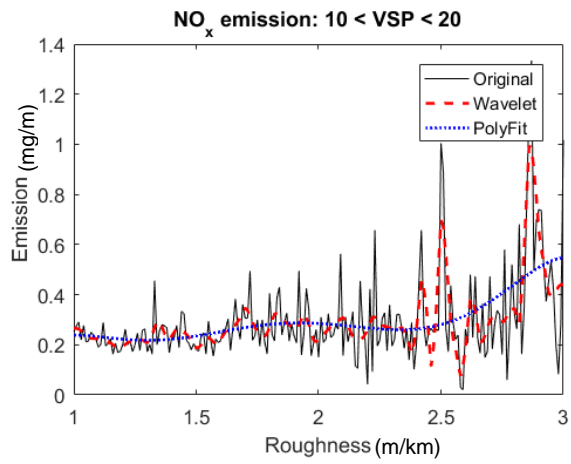
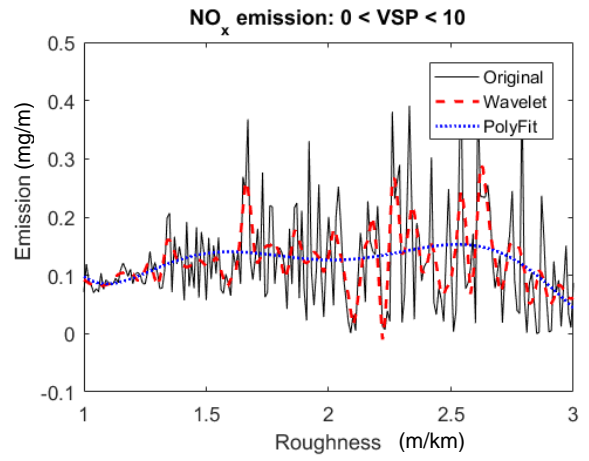
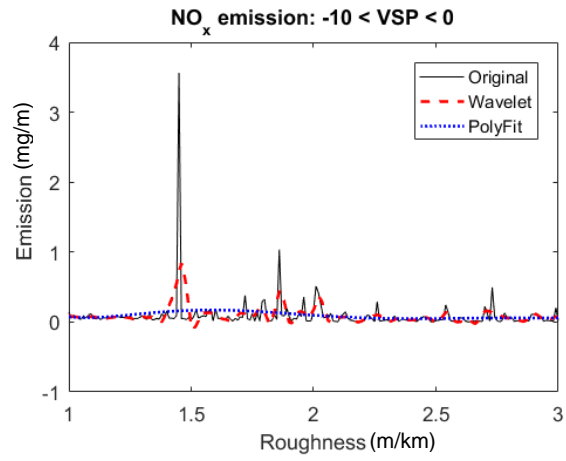
Fig. 4 Comparison between Wavelet Approximation and Polyfit of CO emission for different VSP ranges



233

234

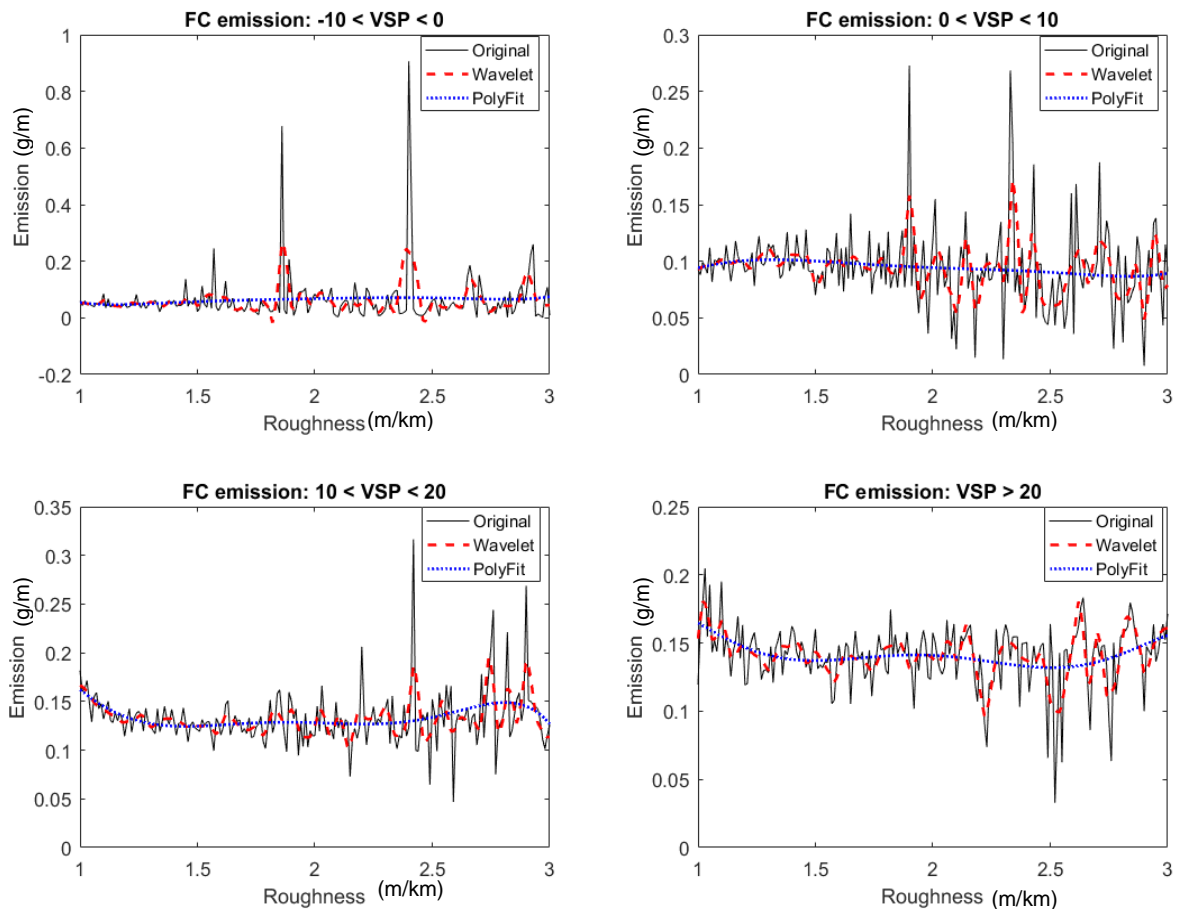
Fig. 5 Comparison between Wavelet Approximation and Polyfit of HC emission for different VSP ranges



235

236

Fig. 6 Comparison between Wavelet Approximation and Polyfit of NO_x emission for different VSP ranges



237

238

Fig. 7 Comparison between Wavelet Approximation and Polyfit of fuel consumption for different VSP ranges

239

A general trend of emissions and fuel consumption can be recognized from above figures. For CO₂, CO and HC emissions and also FC are lower in negative VSP, 0 < VSP < 10 and 10 < VSP < 20 bins for lower pavement roughness and then the emissions become higher as the roughness increases. Only NO_x shows somewhat different trend than the other emissions having larger emissions at the middle range of roughness within negative VSP range. For the bin where VSP > 20, CO₂, NO_x and FC are showing initial spike of emissions for lower roughness and increases again for the higher IRI.

244

245

6.2 Error Measurement for Wavelet Approximations and Polynomial Fitting

246

The Root Mean Square Errors, shown in Eq. (6), from Wavelet approximation analysis and Polynomial curve fitting were calculated for each gas and FC and for every VSP range. The Table 1 shows that the RMSE calculated for Wavelet is less than RMSE calculated for Polyfit. Thus, wavelet approximation

247

248

249 performs better than the polynomial approximation in all five emissions. However, the root mean square
 250 error for both analyses is relatively higher for negative VSP than the positive ones. We believe this is
 251 due to the presence of sharp, large-valued emission peaks that were observed in negative VSP regime.
 252 Our previous study also indicated large emission vs roughness trend for negative VSP and, thus we can
 253 univocally assume that sources of such emissions should be addressed in order to realize more
 254 fuel-efficient transportation.

$$RMSE = \sqrt{\frac{\sum_{i=1}^n (y_{observed} - y_{model})^2}{n}} \quad (6)$$

256 where, n is the number of data and RMSE = Root Mean Square Error

257 **Table 1** RMSE of Wavelet Approximation and PolyFit

Emission	VSP range	Polyfit RMSE	Wavelet RMSE
CO	-10<VSP<0	2.7883	2.4174
	0<VSP<10	0.4506	0.4163
	10<VSP<20	0.5535	0.4421
	VSP>20	0.8739	0.7518
CO₂	-10<VSP<0	0.2799	0.2427
	0<VSP<10	0.1046	0.0866
	10<VSP<20	0.084	0.0719
	VSP>20	0.0677	0.0526
HC	-10<VSP<0	0.0578	0.0419
	0<VSP<10	0.0376	0.0287
	10<VSP<20	0.0422	0.0368
	VSP>20	0.108	0.0871
NO_x	-10<VSP<0	0.2637	0.2380
	0<VSP<10	0.0812	0.0682

	10<VSP<20	0.1592	0.1218
	VSP>20	0.1821	0.1369
FC	-10<VSP<0	0.0895	0.0776
	0<VSP<10	0.0331	0.0274
	10<VSP<20	0.0265	0.0227
	VSP>20	0.0215	0.0166

258 7 Conclusions

259 In this paper, the relatively new technique of wavelet transformation and analysis has been employed to
260 analyze the relation of emission and road roughness profile. The application methods and procedures
261 for performing the analysis have been presented in detail which included the use of approximation
262 signal generated from multi-level discrete wavelet transform. Based on the analysis presented in this
263 paper, it can be concluded that wavelet analysis possesses the ability to perform local analysis on
264 PEMS data to identify emission trends more accurately than other common nonlinear analysis. In
265 addition, it has been shown that the analysis can be done for different VSP to understand the emission
266 trend for different vehicular conditions. Thus, 1D DWT can be considered as an effective means of
267 estimating emissions for highway engineers to plan on reduction of vehicular emissions on road.

268 Acknowledgments

269 The authors acknowledge that this research is supported in part by the National Science Foundation
270 (NSF) under grants #1137732, and the U.S. National Tier 1 University Transportation Center (UTC)
271 TranLIVE #DTRT12GUTC17/KLK900-SB-003. The opinions, findings, and conclusions or
272 recommendations expressed in this material are those of the author(s) and do not necessarily reflect the
273 views of the funding agencies. The authors would also like to thank Shah Mohammad Bahauddin for his
274 invaluable discussion and comments on discrete wavelet transformation.

275 References

276 Caiazzo, F, A. Ashok, I.A. Waltz, S.H.L. Yim, S.R.H. Barrett. Air pollution and early deaths in the United
277 States. Part I: Quantifying the impact of major sectors in 2005. *Atmospheric Environment* 79 (2013):
278 198-208.

279 Environmental Protection Agency, National- Level Greenhouse Gas Inventory (2016), Available
280 at:[https://www.epa.gov/sites/production/files/2016-04/documents/us-ghg-inventory-2016-main-text](https://www.epa.gov/sites/production/files/2016-04/documents/us-ghg-inventory-2016-main-text.pdf)
281 .pdf.

282 Li, Q., F. Qiao, and L. Yu. Clustering Pavement Roughness Based On the Impacts on Vehicle
283 Emissions and Public Health. *Journal of Ergonomics* 2015 (2016).

284 Kalembo, C., M. Jeihani, and A. Saka. Evaluation of the impact of pavement roughness on vehicle gas
285 emissions in Baltimore County. TRB 2012 Annual meeting, CD-ROM, Washington, DC. 2012.

286 Papageorgiou, G.P., and A. Mouratidis. A mathematical approach to define threshold values of
287 pavement characteristics. *Structure and Infrastructure Engineering* 10.5 (2014): 568-576.

288 Veitch, D. Wavelet Neural Networks and their application in the study of dynamical systems.
289 Department of Mathematics University of York UK(2005).

290 Wei, L., T. F. Fwa, and Z. Zhe. Pavement roughness analysis using wavelet theory. In Proceedings from
291 the 6th International Conference on Managing Pavements. Queensland, Australia. 2002.

292 Qiao, F., X. Wang, and L. Yu. Optimizing aggregation level for ITS data based on wavelet
293 decomposition. Preprint CD-ROM, Transportation Research Board (2003).

294 Daubechies, I. Ten lectures on wavelets. Vol. 61. Philadelphia: Society for industrial and applied
295 mathematics, 1992.

296 Qiao, F., H. Liu, and L. Yu. Incorporating wavelet decomposition technique to compress TransGuide
297 intelligent transportation system data. *Transportation Research Record: Journal of the*
298 *Transportation Research Board* 1968, 2006, pp. 63-74.

299 Forslöf, L. and H. Jones. Roadroid: Continuous Road Condition Monitoring with Smart Phones. *Journal*
300 *of Civil Engineering and Architecture*, 2015. Volume 9, pp. 485-496.

301 Jimenez-Palacios, J. L. Understanding and quantifying motor vehicle emissions with vehicle specific
302 power and TILDAS remote sensing. Diss. Massachusetts Institute of Technology, 1998.

303 Greene, Suzanne et al. "Pavement Roughness and Fuel Consumption" MIT Concrete Sustainability

304 Hub (CSHub), Cambridge, MA, Massachusetts Institute of Technology, 2003.

305 Wei, Liu, T. F. Fwa, and Zhao Zhe. "Wavelet analysis and interpretation of road roughness." *Journal of*
306 *transportation engineering* 131.2 (2005): 120-130.

307 Wei, Liu, and T. Fwa. "Characterizing road roughness by wavelet transform." *Transportation Research*
308 *Record: Journal of the Transportation Research Board* 1869 (2004): 152-158.

309 Wei, Liu, and T. F. Fwa. "Application of wavelet transform analysis for pavement roughness studies."
310 *Proceedings of the International Conference on Applications of Advanced Technologies in*
311 *Transportation Engineering* (2004).

312 Zhou, Jian, Peisen S. Huang, and Fu-Pen Chiang. "Wavelet-based pavement distress detection and
313 evaluation." *Optical Engineering* 45.2 (2006): 027007-027007.

314 Nagy, Sz. "On wavelet based modeling of the nitrogen oxides emission and concentration due to road
315 traffic in urban environment." *Acta Technica Jaurinensis* 8.1 (2015): 47-62.

316 Wang, Zhanyong, et al. "Fine-scale estimation of carbon monoxide and fine particulate matter
317 concentrations in proximity to a road intersection by using wavelet neural network with genetic
318 algorithm." *Atmospheric Environment* 104 (2015): 264-272.

319 Forslöf, Lars, and Hans Jones. "Roadroid: continuous road condition monitoring with smart phones."
320 IRF 17th World Meeting and Exhibition, Riyadh, Saudi Arabia. Available from [http://www.roadroid.](http://www.roadroid.com/common/References/IRF)
321 [com/common/References/IRF](http://www.roadroid.com/common/References/IRF). Vol. 202013. 2013.

322 Nabi, M., Qiao, F., and L. Yu. "Quantifying Vehicular Emission Factors With the Impact of
323 Lane-changing Behavior on Different Types of Weaving Segment of Freeways" publication date
324 Aug 24, 2016 publication description 2016 A&WMA Annual Conference & Exhibition Proceedings

325 Khan, M., Qiao, F., and Yu, L. "Wavelet Analysis to Characterize Dependency of Vehicular Emissions
326 on Road Roughness". *Transportation Research Board*, Washington D.C., 2017,
327 <https://trid.trb.org/view.aspx?id=1437622>